Theory of the optical conductivity in the cuprate superconductors

Branko P. Stojković*
Department of Physics and Materials Research Laboratory, 1110 West Green Street, University of Illinois, Urbana, Illinois 61801

David Pines†
Center for Nonlinear Studies, Los Alamos National Laboratory, Los Alamos, New Mexico 87545
(Received 30 May 1997)

We present a study of the normal-state optical conductivity in the cuprate superconductors using the nearly antiferromagnetic Fermi-liquid (NAFL) description of the magnetic interaction between their planar quasiparticles. We find that the highly anisotropic scattering rate in different regions of the Brillouin zone, both as a function of frequency and temperature, a benchmark of NAFL theory, leads to an average relaxation rate of the marginal Fermi-liquid form for overdoped and optimally doped systems, as well as for underdoped systems at high temperatures. We carry out numerical calculations of the optical conductivity for several compounds for which the input spin-fluctuation parameters are known. Our results, which are in agreement with experiment on both overdoped and optimally doped systems, show that NAFL theory explains the anomalous optical behavior found in these cuprate superconductors. [S0163-1829(97)03537-6]

I. INTRODUCTION

Optical conductivity measurements show that high-temperature superconductors (HTS's) exhibit a number of anomalies when compared to the usual Drude-like Fermi-liquid (FL) behavior found in conventional metals. Quite generally, experiment shows that the effective transport scattering rate $1/\tau(\omega)$ exhibits linear-in-ω behavior over a wide frequency range, while the measurements of Puchkov *et al.*[1] demonstrate that significant deviations from this standard behavior occur, especially in underdoped materials at low temperatures, in the so-called pseudogap regime, where $1/\tau(\omega)$ is strongly suppressed. These anomalies are often attributed to a possible non-Fermi-liquid ground state in these materials.[2]

The linear frequency dependence of $1/\tau$ at relatively high ω can be regarded as the optical analog of the anomalous resistivity, $\rho \propto T$, found in the superconducting cuprates, and its presence has been considered as major support for the marginal-Fermi-liquid (MFL) approach.[3] In the MFL approach, the self-energy is given by

$$\Sigma(\mathbf{k},\omega) = \lambda\left(\omega \ln\frac{x}{\omega_c} - i\frac{\pi}{2}x\,\mathrm{sgn}\omega\right), \tag{1}$$

where $x = \max(|\omega|, T)$, ω_c is a cutoff frequency, and λ a coupling constant, an expression which explained many of the early experiments.[4] However, Eq. (1) is inconsistent with recent angular-resolved photoemission spectroscopy (ARPES) experiments[5] on the underdoped materials, which show that both the quasiparticle spectral weight and lifetime are highly anisotropic as one goes around the Fermi surface (FS), rather than being momentum independent as Eq. (1) requires.

Highly anisotropic quasiparticle behavior finds a natural explanation in the nearly antiferromagnetic Fermi-liquid (NAFL) model of cuprates,[6] in which the effective interaction between planar quasiparticles is assumed to be proportional to the dynamic spin susceptibility $\chi(q,\omega)$ measured in NMR and inelastic neutron scattering (INS) experiments. Because $\chi(q,\omega)$ is strongly peaked in the vicinity of the antiferromagnetic wave vector $\mathbf{Q}=(\pi,\pi)$, quasiparticles on the FS located in the vicinity of the hot spots,[7] portions of the FS which can be connected by wave vectors $\sim\mathbf{Q}$, interact strongly, while those located elsewhere (in *cold* regions) interact comparatively weakly.

NAFL theory, with spin-fluctuation parameters and a quasiparticle spectrum taken from experiment, yields results consistent with low-frequency NMR and INS experiments, as well as ARPES measurements of the Fermi surface properties.[5,8] We have recently shown that it also provides a consistent qualitative, and in many cases quantitative, explanation of the measured changes with doping and temperature of both the longitudinal and Hall conductivities of the cuprates, and shown how one can extract the quite distinct lifetimes of ''hot'' and ''cold'' quasiparticles as a function of temperature directly from these measurements.[9] In this paper we consider NAFL theory at infrared frequencies and show that it explains as well the measured anomalous optical behavior.

Our paper is organized as follows. Following a review of the physical properties of NAFL's, we discuss in Sec. III both analytic and numerical calculations of the highly anisotropic quasiparticle lifetime and the quasiparticle relaxation rate at finite frequency ω and temperature T. In Sec. IV we calculate the optical conductivity and discuss its limiting behavior. In Sec. V we use realistic band and spin-fluctuation parameters to compare our results with experiment. Our conclusions are presented in Sec. VI.

II. PHYSICAL PROPERTIES OF NAFL'S

In the NAFL description of the normal-state properties of the superconducting cuprates, it is the magnetic interaction between planar quasiparticles which is responsible for the anomalous spin and charge behavior. The magnetic proper-

ties of the system are specified by the dynamical spin-spin response function of fermionic origin, $\chi(\mathbf{q},\omega)$, which near a peak at a wave vector $\mathbf{Q}_i$ in the vicinity of $\mathbf{Q}$ is assumed to take the mean-field form[10]

$$\chi(q,\omega)=\frac{\chi_Q}{1+(\mathbf{q}-\mathbf{Q}_i)^2\xi^2-i\omega/\omega_{\rm sf}}. \tag{2}$$

Hence $\chi_Q=\alpha\xi^2\gg\chi_0$ is the magnitude of the static spin susceptibility at $\mathbf{Q}_i$, ξ is the antiferromagnetic correlation length, $\omega_{\rm sf}$ specifies the low-frequency relaxational mode, brought about by the near approach to antiferromagnetism, and α is a temperature-independent scale factor. We use a system of units in which the lattice spacing $a=1$. Although experiment suggests that the susceptibility (2) quite generally possesses four peaks at the incommensurate wave vectors $\mathbf{Q}_i\approx\mathbf{Q}$, since the introduction of the incommensuration does not introduce qualitatively new physics, we shall assume for the most part that the spin-fluctuation spectrum possesses only a single peak at $\mathbf{Q}$.

The quasiparticle spectrum is assumed to take a tight-binding form,

$$\epsilon_k=-2t(\cos k_x+\cos k_y)-4t'\cos k_x\cos k_y -2t''[\cos(2k_x)+\cos(2k_y)], \tag{3}$$

where t, t', and t'' are the appropriate hopping integrals, while the effective magnetic interaction between the planar quasiparticles is specified by

$$V_{\rm eff}(\mathbf{q},\omega)=g^2\chi(\mathbf{q},\omega). \tag{4}$$

For a given system the parameters $\chi_{\mathbf{Q}_i}$, ξ, and $\omega_{\rm sf}$ which determine $\chi(\mathbf{q},\omega)$ are taken from fits to NMR and INS experiments, while the effective coupling constant, g, is assumed to be momentum independent for wave vectors near $\mathbf{Q}_i$. As discussed by Chubukov *et al.*,[11] the effective interaction, Eq. (4), can be, in principle, derived microscopically starting with, e.g., a one-band Hubbard model.

The effective interaction $V_{\rm eff}$, Eq. (4), has the obvious property that for sufficiently large correlation lengths it is highly peaked for momentum transfers in the vicinity of the antiferromagnetic wave vector $\mathbf{Q}$. The consequences of this peaking are hard to overestimate: if the FS of the system of fermions, defined by the quasiparticle dispersion (3), is such that it intersects the magnetic Brillouin zone (BZ) (see Fig. 1), then quasiparticles in the vicinity of these intersection points on the FS, the hot spots,[7] are much more strongly scattered by the spin fluctuations than those which are on other parts (cold regions) of the FS. This leads to strongly anisotropic quasiparticle behavior, since the resulting temperature and frequency variation of the quasiparticle scattering rates at and far away from hot spots is in general very different. We shall return to this point in the following section.

Barzykin and Pines (BP) have used Eq. (2) to analyze NMR results in the cuprates.[12] They find that for underdoped systems the low-frequency magnetic behavior possesses three distinct normal-state phases, and that the characteristic frequencies and lengths which enter Eq. (2) are connected by a dynamic scaling relationship $\omega_{\rm sf}\propto\xi^{-z}$ in two of the phases.

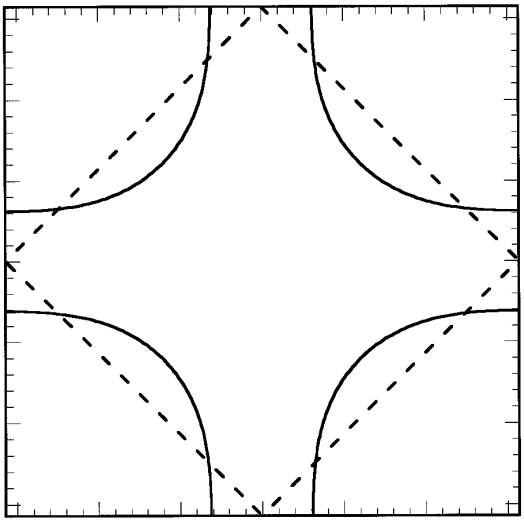

FIG. 1. A model FS in cuprates. For a quasiparticle interaction peaked at $\mathbf{Q}$, the intersection of the magnetic Brilloiun zone (shown with the dashed line) with the FS specifies the singular points at which the interaction is maximally effective in low-energy scattering processes.

Thus, above the temperature $T_{\rm cr}$ at which the temperature-dependent uniform susceptibility $\chi_0(T)$ possesses a maximum, the system exhibits nonuniversal mean field (MF) behavior with dynamical exponent $z=2$, $\omega_{\rm sf}\sim 1/\xi^2$, and the product, $\chi_{\mathbf{Q}}\omega_{\rm sf}\sim\omega_{\rm sf}\xi^2$ is independent of temperature. From a detailed analysis of the NMR experiments, Barzykin and Pines conclude that the crossover temperature $T_{\rm cr}$ is determined by the strength of the AF correlations, with $\xi(T_{\rm cr})\approx 2$. Below $T_{\rm cr}$, down to a second crossover temperature T_*, underdoped systems exhibit nonuniversal, $z=1$, pseudoscaling (PS) behavior. Thus, for $T_*\leqslant T\leqslant T_{\rm cr}$, it is $\omega_{\rm sf}\xi$ which is independent of temperature. NMR experiments show that above $T_{\rm cr}$, in the MF regime, $\omega_{\rm sf}$ and $1/\xi^2$ scale linearly with T, i.e., $\omega_{\rm sf}=A+BT$, while in the PS regime, between T_* and $T_{\rm cr}$, it is $\omega_{\rm sf}$ and ξ^{-1} which scale linearly with T, albeit with a possibly somewhat different slope and intercept of $\omega_{\rm sf}$ than that found above $T_{\rm cr}$. This behavior has now been verified experimentally for the $YBa_2Cu_3O_{7-x}$, $La_{2-x}Sr_xCuO_4$ (x is the hole doping level), and $YBa_2Cu_4O_8$ systems,[12] as well as the Hg and 2212 BSCCO compounds.[13] Below T_*, in the pseudogap (PG) regime, ξ becomes independent of temperature while $\omega_{\rm sf}$, after exhibiting a minimum near T_*, rapidly increases (roughly as $1/T$) as T decreases toward T_c. These changes in the magnetic fluctuation spectrum are accompanied by (indeed result from) changes in the quasiparticle spectrum.[11] Thus, the PS regime is characterized by a strong temperature variation of the quasiparticle spectrum, resulting in a FS evolution[11] which has nontrivial consequences for the transport properties of underdoped systems.[9] The crossovers seen in the low-frequency magnetic behavior thus possess, to a considerable extent, their charge counterparts in transport experiments.

From a magnetic perspective, the so-called optimally doped systems (e.g., $YBa_2Cu_3O_{6.93}$ and $La_{1.85}Sr_{0.15}CuO_4$) are a special case of the underdoped systems, in which T_* is comparatively close to T_c. Overdoped cuprates are defined as those for which $T_{\rm cr}<T_c$. For these systems, then, the

antiferromagnetic correlations are comparatively weak, with $\xi \leqslant 2$, and $\chi_0(T)$ is at most weakly temperature dependent, while $\omega_{\rm sf} \propto \xi^{-2}$ follows the linear-in-T behavior found in the underdoped systems above $T_{\rm cr}$. Examples of overdoped systems are the $T_c \sim 40$ K Tl 2212 system and $La_{2-x}Sr_xCuO_4$ for $x \geqslant 0.24$.

As Monthoux and Pines[14] and Chubukov *et al.*[11] have emphasized, the physical origin of the highly anomalous behavior displayed by the nearly antiferromagnetic Fermi liquids resides in the nonlinear feedback of changes in the *hot* quasiparticle spectrum on the strong quasiparticle interaction, $\sim \chi(\mathbf{q},\omega)$, which determines that *hot* quasiparticle behavior. For systems above $T_{\rm cr}$, or in overdoped systems, that feedback is negative; strong-coupling effects cause $\chi_0(T)$ to increase weakly as the temperature decreases, while a random phase approximation (RPA) or mean-field description suffices to determine the relationship between $\omega_{\rm sf}$ and ξ. At a critical value of the strength of the AF correlations, that feedback becomes positive; a weak pseudogap develops in the hot quasiparticle spectrum, bringing about a linear decrease in $\chi_0(T)$ as T decreases below $T_{\rm cr}$, while the quasiparticle damping of spin excitations becomes T dependent in such a way that $\omega_{\rm sf}$ displays $z=1$ pseudoscaling behavior, with the strength of the AF correlations, ξ, growing as $(a+bT)^{-1}$. The second crossover temperature T_* marks the transition to ''strong'' pseudogap behavior: The AF correlations become frozen; $\omega_{\rm sf}$ increases rapidly as T decreases below T_*, while $\chi_0(T)$ falls off rapidly between T_* and T_c. It is the interplay between these changes in the quasiparticle spectrum (seen directly in ARPES measurements) and the spin fluctuation spectrum, and effective quasiparticle interaction, seen directly in NMR and INS experiments, which is responsible for the anomalous quasiparticle lifetimes we now consider.

III. QUASIPARTICLE LIFETIME AT FINITE FREQUENCY

We begin by estimating the effective scattering rate, for quasiparticles near the FS, as a function of frequency and temperature using simple perturbation theory. The quasiparticle lifetime is determined by the imaginary part of the single-particle self-energy, which, for the effective interaction (4), in the second-order Born approximation, reads

$$\mathrm{Im}\Sigma(k,\omega) = \sum_{k'} g^2 \mathrm{Im}\chi(\mathbf{k}-\mathbf{k}', \omega-\epsilon') \times [n_0(\epsilon'-\omega) + f_0(\epsilon')], \tag{5}$$

where $\epsilon' \equiv \epsilon_{k'}$, and $n_0(\epsilon)$ and $f_0(\epsilon)$ are the Bose and Fermi distribution functions, respectively. The transport relaxation rate is usually given by

$$\frac{1}{\tau_k(\omega)} = \int \frac{d^2k'}{(2\pi)^2} 2g^2 \mathrm{Im}\chi(\mathbf{k}-\mathbf{k}', \epsilon'-\omega)[n_0(\epsilon'-\omega) + f_0(\epsilon')](1-\gamma_{k,k'}), \tag{6}$$

where $\gamma_{k,k'}$ is a temperature-independent vertex function which removes forward-scattering processes from the calculated transport relaxation rate. As we shall see below, for overdoped, optimally doped, and even underdoped systems above T_*, the dominant contribution to $1/\tau_k$ comes from large momentum transfer scattering processes and hence the use of $\gamma_{k,k'}$ for forward-scattering corrections plays only a minor role. Therefore we assume $\gamma = 0$, and return later to the role of the vertex corrections at low temperatures in underdoped systems.

We make the usual change of variables in the integral in Eq. (6):

$$\int d^2k' \to \int d\epsilon' \int \frac{dk'}{|\mathbf{v}|}, \tag{7}$$

where k' is the component of momentum $\mathbf{k}'$ parallel to the equipotential lines ($\epsilon' = \text{const}$), and carry out the integration over ϵ' for $\mathbf{k}$ near the FS and $\epsilon \ll t$, where t is the hopping matrix element. On making the substitution $x = (\epsilon' - \omega)/T$ in Eq. (6), it becomes

$$\frac{1}{\tau_k(\omega,T)} = 2\alpha g^2 \omega_{\rm sf} \xi^2 \int_{\rm FS} \frac{dk'}{4\pi^2} I(\mathbf{k},\mathbf{k}',\varepsilon), \tag{8}$$

where

$$I(\mathbf{k},\mathbf{k}',\varepsilon) = \int dx \left[\frac{1}{\exp(x)-1} + \frac{1}{\exp(x+\varepsilon)+1} \right] \frac{x}{\Omega^2 + x^2} \tag{9}$$

and

$$\varepsilon = \omega/T \quad \Omega = \omega_{\rm sf}[1 + \xi^2(\mathbf{k}-\mathbf{k}'-\mathbf{Q})^2]/T \equiv \omega_{k,k'}/T. \tag{10}$$

Note that the definition (10) effectively removes the temperature from the calculation.

Obviously, the integral I is hard to solve analytically. However, we can obtain its value in appropriate limits, and then map its behavior with a universal function which possesses the correct limiting values.

Low frequency limit, $\varepsilon \ll 1$: In this limit one can expand $1/[\exp(x+\varepsilon)+1]$ in Eq. (9). The first nonvanishing correction to $I(\varepsilon = 0)$ is $I_2 \varepsilon^2$, where

$$I_2 = \frac{1}{2} \int_{-\infty}^{\infty} dx \frac{x}{x^2+\Omega^2} \frac{\partial^2}{\partial x^2} \left(\frac{1}{\exp(x)+1} \right). \tag{11}$$

When $\Omega \ll 1$ one finds $I_2 = 7\zeta(3)/2\pi^2 - \pi\Omega/8$ to lowest order in Ω, while in the limit $\Omega \gg 1$ one finds $I_2 \approx 1/\Omega^2$ to lowest order in $1/\Omega$.

Low-temperature limit, $\varepsilon \gg 1$, $\Omega \gg 1$: In this limit, to leading order in $1/\varepsilon$ and $1/\Omega$ Eq. (9) becomes

$$I(\varepsilon) = \frac{1}{2} \ln\left(1 + \frac{\varepsilon^2}{\Omega^2}\right) + \frac{\pi^2}{6} \frac{\Omega^2 - \varepsilon^2}{(\Omega^2+\varepsilon^2)^2} + \frac{\pi^2}{3\Omega^2}. \tag{12}$$

The first term in Eq. (12) is the zero-temperature result which correctly incorporates the above small-ε behavior. The remaining two terms are of order T^2, as in usual FL's. If the temperature is increased while $\varepsilon \gg 1$ is maintained, then the result depends on Ω in a nontrivial way: A quick check reveals that in the $\Omega \ll 1$ limit $I \approx \pi/\Omega$, as in the zero-frequency case.

If one seeks a universal function for I, it is not difficult to see that an appropriate form, for all relevant values of Ω and ϵ, is

$$I(\varepsilon)=\frac{1}{2}\ln\left(1+\frac{\varepsilon^2}{\Omega^2}\right)+\frac{\pi^2}{2\Omega(\Omega+\pi)}. \tag{13}$$

This function displays the correct limiting behavior for both low and high frequencies and temperatures. As a function of Ω it has a crossover from $1/\Omega$ to $1/\Omega^2$ behavior, reflecting the fact that as a function of temperature I displays a crossover from $(\pi T)^2/\omega_{kk'}^2$ at low temperatures to $\pi T/\omega_{kk'}$ at high temperatures [see Eq. (10)].

The result (13) leads to the correct behavior of the scattering rate in the case of typical metallic conductors, for which the relevant energy scale $\omega_{kk'}$ is of order Fermi energy E_f, $\omega_{k,k'}$ is weakly momentum dependent, and $\Omega\sim E_f/T\gg 1$ for all k and k'. On using Eqs. (12) and (13), one trivially recovers the FL result

$$\frac{1}{\tau}\propto\frac{\omega^2+(\pi T)^2}{E_f^2}. \tag{14}$$

It is important to realize that the form of the integral I in Eq. (13) is such that one can treat the dependence on frequency and on temperature almost independently. When ε and Ω are of comparable size, the second term in Eq. (12) is small compared to the third, and finds a result, which, although differing somewhat from Eq. (13),

$$I(\varepsilon)=\frac{1}{2}\ln\left(1+\frac{\varepsilon^2}{\Omega^2}\right)+\frac{\pi^2}{3\Omega(\Omega+\pi/3)}, \tag{15}$$

turns out to be correct for a wide variety of experimentally relevant parameters. For Eq. (15) the crossover from π/Ω behavior at $\Omega\ll 1$ to π^2/Ω^2 behavior at $\Omega\gg 1$ occurs at considerably lower values of Ω than is the case with Eq. (13).

For the case at hand, for which $\omega_{kk'}\leqslant kT$, we follow Refs. 9 and 15 and carry out the integration over k' in Eq. (8) by making the approximation

$$\omega_{kk'}\approx\omega_{\rm sf}[1+\xi^2(\Delta k')^2+\xi^2(\Delta k)^2], \tag{16}$$

where $\Delta k'$ and Δk measure the displacements of k and k' from the corresponding adjoint hot spots along the FS. Then, for doping levels such that one has a large FS, to a high degree of numerical accuracy, the integral over $\Delta k'$ can be extended to infinity, and for a general point near the FS the scattering rate is given by

$$\frac{1}{\tau_k(\omega)}=\frac{\alpha g^2\xi\sqrt{\omega_{\rm sf}}}{2\pi v_f}(F_k^{\epsilon}+F_k^T) \tag{17}$$

where

$$F_k^T=\frac{\pi T}{2}\left[\frac{1}{\sqrt{\omega_{\rm sf}[1+\xi^2(\Delta k)^2]}}-\frac{1}{\sqrt{\pi T+\omega_{\rm sf}[1+\xi^2(\Delta k)^2]}}\right] \tag{18}$$

and

$$F_k^{\epsilon}=\sqrt{2}\sqrt{\sqrt{\omega_{\rm sf}^2[1+\xi^2(\Delta k)^2]^2+\omega^2}+\omega_{\rm sf}[1+\xi^2(\Delta k)^2]}-2\sqrt{\omega_{\rm sf}[1+\xi^2(\Delta k)^2]}. \tag{19}$$

The behavior of F_k^T, which determines the low-frequency, ω-independent limit of $1/\tau_k(\omega)$, has been discussed in some detail in Ref. 9; we turn therefore to the behavior of F_k^{ϵ} in various limiting cases.

Finite (but low) frequencies, $\omega\ll\omega_{\rm sf}$: As indicated by the $\varepsilon\to 0$ behavior of integral $I(k,k',\varepsilon)$ above, the low-frequency correction to the (temperature-induced) scattering rate is always proportional to $\varepsilon^2\propto\omega^2$, as in ordinary FL's. However, unlike Landau Fermi liquids, from Eqs. (19) one finds that the coefficient of proportionality, α_k, is strongly momentum dependent:

$$1/\tau_k(T,\omega)-1/\tau_k(T,\omega=0)\approx\frac{\alpha g^2}{2\pi v_f}\frac{\sqrt{\omega_{\rm sf}}\xi}{4\omega_{\rm sf}^{3/2}[1+\xi^2(\Delta k)^2]^{3/2}}\omega^2\equiv\alpha_k\omega^2. \tag{20}$$

For hot quasiparticles with $\Delta k\xi\ll 1$, the characteristic energy scale which determines this FL-like behavior is small, being $\sim\omega_{\rm sf}$, while for cold quasiparticles, with $\Delta k\xi\gg 1$, it is much larger, $\sim\omega_{\rm sf}\xi^2(\Delta k)^2$. Hence, in the cold regions $1/\tau$ is proportional to ω^2 up to rather high frequencies of order $\omega_{\rm sf}\xi^2\sim 100$ meV. This result has important consequences: Although the range of frequencies where the FL-like scattering rate persists is very small in the hot regions, one can use FL theory to calculate the effective mass $m^*=m(1-\partial\Sigma'/\partial\omega)$, which may be large, but is always finite. For cold quasiparticles one finds a comparatively modest effective mass enhancement at all temperatures of interest.

Intermediate frequencies, $\omega_{\rm sf}\ll\omega\ll\omega_{\rm sf}\xi^2$: It follows from Eq. (19) that the hot quasiparticles possess a lifetime

$$\frac{1}{\tau_k}\approx\frac{1}{\tau_k(\omega=0)}+\frac{\alpha g^2}{2\pi v_f}\sqrt{2\omega\omega_{\rm sf}\xi^2}, \tag{21}$$

while for cold quasiparticles, as long as $\omega\ll\omega_{\rm sf}\xi^2(\Delta k)^2$, Eq. (20) still holds.

Intermediate frequencies, $\omega\sim\omega_{\rm sf}\xi^2(\Delta k)^2$, $\Delta k\leqslant 1$: From Eq. (19) it is also relatively easy to obtain a simple expression for the cold quasiparticle lifetime at intermediate values of frequency and Δk, such that $\omega\sim\omega_{\rm sf}\xi^2(\Delta k)^2$:

$$\frac{1}{\tau_k}-\frac{1}{\tau_k(\omega=0)}\approx\frac{\alpha g^2}{2\pi v_f}\frac{\eta\omega}{\Delta k}, \tag{22}$$

where η is a numerical coefficient of order 0.7. On combining Eqs. (20) and (22) and making use of our previous results for $1/\tau_k(\omega=0)$, we see that, to a good degree of accuracy, we can write

$$\frac{1}{\tau_k(\omega,T)}\approx\frac{\alpha g^2}{4v_f\Delta k}\left(\frac{(\pi T)^2}{\pi T+\pi T_0(k)}+\frac{\omega^2}{\omega+E_0(k)}\right), \tag{23}$$

where

$$\pi T_0(k)\sim E_0(k)\sim 2\omega_{\rm sf}\xi^2(\Delta k)^2. \tag{24}$$

The quantities πT_0 and E_0 are not identical, but are nevertheless of comparable magnitude. Hence we see, as might expected for any interacting FL, that the same energy scale $E_0(k)$ (up to a multiplicative constant of order π) determines the crossover from FL behavior at low ω and T to a non-Fermi-liquid linear-in-ω and -T regimes. The crossover frequency increases somewhat with increasing temperature if, as is the case in overdoped materials, ω_{sf} no longer plays a negligible role in determining $1/\tau_k(\omega)$. In this case E_0 is large and $1/\tau$ is only weakly frequency dependent.

As in the case of the dc resistivity, one expects the dominant scattering rates for the optical conductivity to be those of the relatively well-defined quasiparticles in the cold regions of the BZ; the corresponding values of Δk lie within a range $\Delta k \sim 1-2$ for an overdoped material.[9] For an underdoped material Δk is much smaller, $\Delta k < 0.5$, since the FS is not only close to the magnetic BZ boundary, but there may be strong incommensuration effects. In addition, while in the overdoped materials $\omega_{sf}\xi^2 = \text{const}$ as required by the $z=2$ scaling, in underdoped materials one encounters the $z=1$ scaling relationship between the characteristic energy and momenta, where $\omega_{sf}\xi = \text{const}$ and $\xi \sim 1/T$.

A key feature of the NAFL model is that the relevant scale for the frequency and temperature variation of the relaxation rates, $E_0 = \omega_{sf}\xi^2(\Delta k)^2_{max}/\pi$, is considerably smaller than the fermionic bandwidth. Hence at practically any frequency of interest (say, $\omega > 10$ meV) and in the temperature regime where the resistivity is linear in T one finds from Eq. (17) that the *momentum average* scattering rate as a function of frequency and temperature takes the MFL form

$$\left\langle \frac{1}{\tau} \right\rangle_k \approx \frac{\alpha g^2}{4\pi v_f}(\omega + \pi T). \tag{25}$$

Thus, the NAFL approach leads to the major result of MFL theory[3] without resorting to a model in which [see Eq. (1)] one encounters an infinite effective mass of the quasiparticles; indeed, as noted above, in the NAFL model the effective mass of the cold quasiparticles is always of the order of unity.

Equation (23) implies a parallel between the T and ω dependence of the scattering rates: Since the same characteristic frequencies appear in both cases,[9] the behavior of $1/\tau$ as a function of ω or T is approximately the same. We verify this in Fig. 2 where we plot the zero-temperature scattering rate as a function of ω at fixed large ξ and $\omega_{sf} \to 0$ for several values of Δk near the FS. The top panel shows quasiparticle scattering rates when the FS is large [Eq. (21)], while the bottom panel displays our result for a small effective FS with a maximum distance from a singular point along the FS of $\Delta k_{max} = 0.3$. In the latter case the integral over k' in Eq. (8) was done numerically. The corresponding scattering rates as a function of temperature at zero frequency are given in the insets of the panels. The parallel between the zero-frequency temperature and zero-temperature frequency dependences of the scattering rate is quite obvious. Clearly, the rate is highly anisotropic as a function of momentum and decreases dramatically as one departs from the singular point, $\Delta k = 0$, where it is the largest and most anomalous, $1/\tau \sim \sqrt{\omega}$. On the other hand, we notice that the influence of the FS size is felt

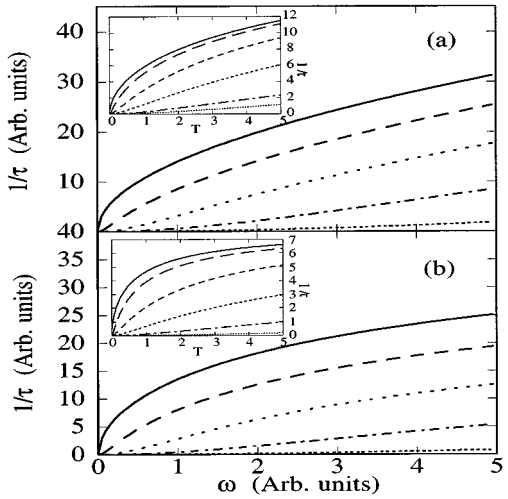

FIG. 2. The frequency dependence of the quasiparticle scattering rate at $T=0$ in (a) the case of a large FS and (b) the case of a small FS, for which $\Delta k_{max} = 0.3$. In both panels the curves correspond to (from top to bottom) $\Delta k = 0$, 0.1, 0.25, 0.5, 1. The insets show the corresponding results at zero frequency as a function of temperature.

mostly in the hot regions while cold quasiparticle lifetimes are comparatively insensitive to the size of the FS.

We consider next the influence of changes in the spin fluctuations spectrum on the quasiparticle scattering rate. We begin with systems and temperatures which display $z=2$ scaling, where $\omega_{sf}\xi^2$ does not depend on temperature. As explained in Sec. II, this scaling law is observed in NMR measurements on overdoped systems or underdoped systems at temperatures above T_{cr}. In Fig. 3(a) we show the frequency dependence of the hot quasiparticle scattering rate for several different temperatures. In order to make the connection with experiment, in this, and many subsequent figures we plot the inverse mean free path in the units of lattice spacing, by assuming a constant Fermi velocity, $v_f = 0.25$ eV. As in previous work,[9] we have assumed realistic spin-fluctuation parameters[16] appropriate for $YBa_2Cu_3O_7$, $\omega_{sf} = [6 + 0.06\,T\,(\text{K})]$ meV and $\omega_{sf}\xi^2 = 60$ meV. We see that the shape of the curve is somewhat less anomalous than that shown in Fig. 2. Since the onset of the non-FL frequency dependence is at $\omega \sim \omega_{sf}$ for a hot spot, the observed behavior is a natural consequence of using a finite value of ω_{sf} and a correspondingly modest value of ξ. Since ω_{sf} increases with temperature the scattering rate becomes even more FL-like at higher temperatures. Quite generally, outside of the pseudogap regime, the behavior of hot quasiparticles becomes less anomalous as T increases, since the system is further away from the AF instability, as measured directly by the size of $1/\xi$ and/or ω_{sf}. Nevertheless, a close inspection shows that the behavior of $1/\tau(\omega)$ is sublinear, i.e., $1/\tau \propto \omega^a$ where $a < 1$.

Figure 3(b) shows the comparable result for cold quasiparticles: we display the average scattering rate averaged over values of Δk, such that $0.5/\xi < \Delta k < 2/\xi$, for the same temperatures as in Fig. 3(a). This average scattering rate is a good measure of the effective relaxation rate, $1/\tau_{eff}(\omega)$, seen in optical measurements, since the behavior of quasiparticles

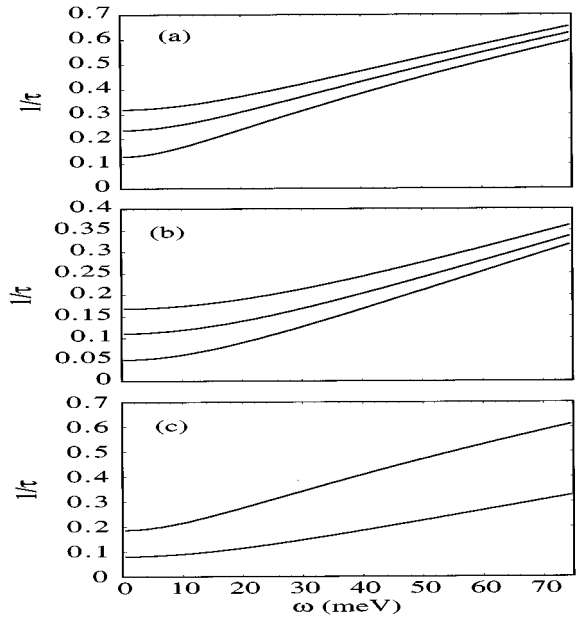

FIG. 3. The frequency dependence of the quasiparticle inverse mean free path (in units of inverse lattice spacing), calculated for $\hbar v_f = 0.25$ eV, at (from bottom to top) $T = 100$, 200, and 300 K. The spin-fluctuation parameters ($\omega_{sf} = [6 + 0.06\,T$ (K)] meV, $\omega_{sf}\xi^2 = 60$ meV) are appropriate for $YBa_2Cu_3O_7$. Panel (a) shows the case with $\Delta k = 0$ (hot region); panel (b) shows the momentum-averaged inverse mean free path for cold quasiparticles ($0.5/\xi < \Delta k < 2$); in panel (c) we compare the frequency dependences of this averaged cold quasiparticle mean free path (bottom) with that of hot quasiparticles (top) at $T = 150$ K. Note the separability of the T and ω contributions to the scattering rate in panels (a) and (b).

at intermediate values of Δk, i.e., $(\Delta k)_{max} \sim 0.5$–1, dominates the transport. Aside from numerical value, which is considerably reduced from that found at the hot spots [see Fig. 3(c)], we see that the behavior is FL-like up to a frequency of order 15 meV, becoming linear with increasing ω. There is no sign of sublinear behavior in $1/\tau$.

In Fig. 3(c), we have plotted the relaxation times for both hot and cold quasiparticles in $YBa_2Cu_3O_7$ at $T = 150$ K, in order to demonstrate the considerable variation in quasiparticle behavior as one moves around the Fermi surface: The frequency dependences of the hot and cold quasiparticle lifetimes are seen to be both qualitatively and quantitatively different. Hot quasiparticles possess a mean free path of order of a few lattice spacings and are comparatively ill defined at higher ω, while in the cold regions of the FS we find very well defined quasiparticles, with mean free paths of up to ten lattice spacings. Note that the mean free path is proportional to v_f^2 and hence is rather sensitive to the choice of this parameter. Our choice of $v_f = 0.25$ eV is somewhat conservative, and the exact value of the mean free path is probably somewhat larger than that displayed in the figure.

We note that, due to the FL-like behavior at low frequency, the behavior of $1/\tau(\omega)$ for cold quasiparticles at different temperatures becomes increasingly more distinct as T increases. This is in sharp contrast with the behavior observed in the singular (hot) region, especially when ξ acquires the temperature dependence appropriate to the $z = 1$ scaling case. This is shown in Fig. 4(a), where we plot our result using spin-fluctuation parameters appropriate for the underdoped $YBa_2Cu_4O_8$ material.[12] The temperature dependence of $1/\tau$ is now completely suppressed at higher frequencies and eventually even inverted from the conventional FL behavior, especially at larger T. By contrast, for the cold quasiparticles, as shown in Fig. 4(b), we obtain results which are very similar to those shown in Fig. 3(b). In Sec. IV we will show that these results lead to the observed optical properties in HTS's.[1] In particular we show that $1/\tau_{eff}$ is linear in ω regardless of the scaling law and hence, provided that the vertex corrections are not large, transport in underdoped materials above T_* is very similar to that in optimally doped materials.

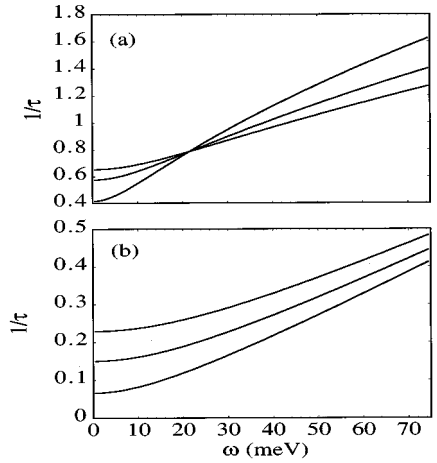

FIG. 4. The quasiparticle inverse mean free path as a function of ω at (from bottom to top, on the left-hand side) $T = 100$, 200, and 300 K in an underdoped material. The spin-fluctuation parameters ($\omega_{sf} = [3.4 + 0.043\,T$ (K)] meV, and $\xi = 50$ meV $/\omega_{sf} \approx 0.07 + 0.00086\,T$ (K)) are appropriate for the pseudoscaling regime in a $YBa_2Cu_4O_8$ sample. Panels (a) and (b) correspond to the hot and momentum-averaged cold regions. Note the unusual temperature dependence of $1/v_f\tau$ at high frequency for the hot quasiparticles.

IV. OPTICAL CONDUCTIVITY

We now turn to the optical conductivity. We begin with the Kubo formula and the well-known expression for the optical conductivity in the absence of the vertex corrections:[17]

$$\sigma_{\mu\nu}(\omega) = \frac{ie^2}{2\pi^2\omega N_k}\sum_k v_k^\mu v_k^\nu \int d\omega' d\omega'' A_k(\omega') A_k(\omega'') \times \frac{f(\omega') - f(\omega'')}{\omega - \omega' + \omega'' - i0_+}, \tag{26}$$

where N_k is the number of points in the BZ and $v_k = \nabla \epsilon_k$, which in the case of a fourfold-symmetric system, where x and y directions are equivalent, yields for the real part of $\sigma_{xx}(\omega)$,

$$\mathrm{Re}\sigma_{xx}(\omega)=\frac{e^2}{4\pi N_k}\sum_k v_k^2\int d\omega' A_k(\omega')A_k(\omega'+\omega)\times\frac{f(\omega')-f(\omega'+\omega)}{\omega}. \quad (27)$$

One can, of course, obtain $\mathrm{Im}\sigma$ using the Kramers-Kronig relations. In Eqs. (26) and (27) $A_k(\omega)$ is the single-particle spectral function,

$$A_k(\omega)=\frac{|\mathrm{Im}\Sigma_k(\omega)|}{[\omega-\epsilon_k-\mathrm{Re}\Sigma_k(\omega)]^2+[\mathrm{Im}\Sigma_k(\omega)]^2}, \quad (28)$$

and $\Sigma_k(\omega)$ is the single-particle self-energy.

In general, Eq. (27) is hard to solve analytically. However, depending on the properties of the self-energy, various approximations can be used. For example, if the self energy is only weakly momentum and frequency dependent, one can use the relaxation time approximation[17]

$$\sigma_{xx}(\omega)=\frac{e^2}{N}\sum_k v_k^2\frac{1}{1/\tau_k(\epsilon_k)-i\omega}\left(\frac{\partial f}{\partial\epsilon}\right), \quad (29)$$

which is the result one obtains using the Boltzmann transport theory. It has been argued that qualitatively the optical properties of cuprates can be captured within this formalism, although assuming a weak dependence of $\Sigma(k,\omega)$ on k and ω clearly represents a considerable oversimplification.

An interesting result can be obtained from Eq. (29). On performing the appropriate integrals, at low T, we find that

$$\mathrm{Re}\sigma_{xx}=e^2\frac{CT}{\omega^2}\ln\left[1+\left(\frac{K_{\max}\omega}{CT}\right)^2\right] \quad (30a)$$

and

$$\mathrm{Im}\sigma_{xx}=e^2\left(\frac{K_{\max}}{\omega}+CT\tan^{-1}\frac{CT}{K_{\max}\omega}-CT\frac{\pi}{2}\right), \quad (30b)$$

where $C=4v_f/\alpha g^2$. We see that, in contrast to ordinary FL's, in NAFL's the real part of σ_{xx} at high frequency depends only weakly on temperature. This weak temperature dependence of $\sigma_{xx}(\omega)$ at high frequency is a generic feature of any system with a low-energy soft mode, be it a NAFL, as above, or a system near a charge density wave instability. Note that Eq. (30) reduces to the appropriate FL results in the $\omega\to 0$ limit.

A generalization of the relaxation time approximation, the memory function formalism,[18] is appropriate for a self-energy which, in the vicinity of the FS, does not depend on momentum, as is the case when the dominant scattering mechanism is due to phonons, as in ordinary metallic superconductors; at sufficiently high frequency, it leads to a Drude-like conductivity

$$\sigma_{xx}(\omega)=\frac{ne^2}{1/\tau_{\mathrm{eff}}(\omega)-i\omega\lambda(\omega)}, \quad (31)$$

with a frequency-dependent effective scattering rate and a frequency-dependent mass m_*, $m_*=m_e[1+\lambda(\omega)]$. This expression is not directly applicable for the case of highly anisotropic scattering rates such as those studied here. However, we show below that in NAFL's, at sufficiently high frequencies, one can obtain an expression of this form, in which $1/\tau_{\mathrm{eff}}$ represents an average scattering rate as a function both of momentum and frequency.

We proceed in the following way: We first recall that in the NAFL model the imaginary part of the self-energy depends only weakly on the component of the wave vector k perpendicular to the FS; the dominant momentum dependence comes from the component which lies in a direction parallel to the FS [see Eq. (19) and the discussion which follows]. This is clearly an approximation, but not an unreasonable one, since only quasiparticles in a narrow region (of order T) around the FS are involved in the scattering [see Eq. (27)]. In this case one can perform the change of variables (7) and integrate over ϵ' explicitly. If the integral can be extended to infinity, the result can be expressed in the quite compact form

$$\mathrm{Re}\sigma_{xx}(\omega)=\frac{e^2}{8\pi^2}\int_{\mathrm{FS}}\frac{dk}{|v_f|}\int d\omega'\frac{f(\omega')-f(\omega'+\omega)}{\omega}\times\mathrm{Im}\left(\frac{v_f^2}{\omega-\Sigma_k(\omega+\omega')+\Sigma_k^*(\omega')}\right). \quad (32)$$

In the limit $\omega\tau\gg 1$ we can expand this expression and compare our result to the Drude formula in the same limit. We find

$$\frac{1}{\tau_{\mathrm{eff}}(\omega)}=\int_{\mathrm{FS}}\frac{dk}{2}\int d\omega'\frac{f(\omega')-f(\omega'+\omega)}{\omega}\times\left(\frac{1}{\tau_k(\omega+\omega')}+\frac{1}{\tau_k(\omega')}\right). \quad (33)$$

In the limit $\omega\gg T$ this yields

$$\frac{1}{\tau_{\mathrm{eff}}(\omega)}=\left\langle\frac{1}{\tau_k}\right\rangle_{\omega,k}, \quad (34)$$

where the angular brackets indicate the appropriate average. We have already obtained the momentum-averaged scattering rate, Eq. (23), which, at high frequencies, took the MFL form, Eq. (25). These expressions show that the average (over momentum) of $1/\tau_k$ is a simple power law as a function of frequency, being quadratic and linear at low and high ω, respectively. As a result, averaging over frequency will not qualitatively change the frequency dependence of the momentum-averaged scattering rate $\langle 1/\tau_k\rangle_k$, since an average of a power-law function is that same function. Therefore, aside from numerical factors (of order 2) and a somewhat different crossover scale E_0, the momentum-averaged scattering rate $\langle 1/\tau_k\rangle_k$ is a reasonable approximation for $1/\tau_{\mathrm{eff}}(\omega)$ in the limit $\omega\tau_{\mathrm{eff}}\gg 1$.

Several important conclusions can be drawn from this result. First, only at high frequencies should the Drude formalism be used to analyze experiments. But, since at sufficiently high frequencies, in general, the quasiparticle picture breaks down, the results we obtain are likely only qualitative. One can show that Drude-like behavior is maintained as one goes to lower frequencies, but the corresponding scattering rate is no longer simply related to the quasiparticle self-energy, and will not be frequency independent. Moreover, quite importantly, in the limit $1/\omega\tau\ll 1$ any feature seen in experiments,

such as the weak temperature dependence of $1/\tau_{\rm eff}(\omega)$ at higher T and ω, or even the pseudogap seen in underdoped materials, must stem from the quasiparticle lifetimes analyzed in the previous section, since it is their average which is probed.

V. COMPARISON WITH EXPERIMENT

We now compare our results with experiment, in order to test the applicability of NAFL theory when one uses realistic parameters for both the effective interaction and band parameters and carries out the relevant integrals numerically. Since the optical conductivity as a function of frequency frequently appears featureless, it is customary to use the memory function formalism[1] to extract the effective transport scattering rates from experiments. Where this has been done, the analysis of the previous section allows us to compare directly our (averaged) scattering times with experiment.

For systems for which the scattering rates have not been determined we compare our calculated values of $\sigma_{xx}(\omega)$ directly to experiment. In so doing, we make use of our numerical results for the optical conductivity obtained by substituting the self-energy (5) into Eq. (27), with and without including the inclusion of the vertex $\gamma_{k,k'}=\cos\theta$ for $1/\tau_k$ where θ is the angle between k and k'. Strictly speaking, this form of the vertex correction is only applicable if the effective interaction is weakly frequency dependent, since only then is the current vertex proportional to the current, and hence additive to the self-energy. In NAFL's this is a somewhat questionable approximation, but as long as $qv_f \ll 1$, while $V_{\rm eff}$ is highly peaked near Q and the FS is large, the magnitude of the vertex correction turns out to be comparatively small, leading to corrections of order 10% for systems near optimal doping. However, since it is straightforward to include it numerically, we retain the function $\gamma_{k,k'}$ in the subsequent numerical results.

We begin with overdoped materials. While it is extremely important to compare the calculated optical conductivity with experiment only for the samples which are used to determine the spin-fluctuation parameters, NMR and optical experimental results on the same sample are often not available. Thus for the first sample we consider, single layer Tl 2201, the samples used by Puchkov *et al.*,[1] for optical experiments had a $T_c=15$ K, while the best available NMR experiments on a comparable sample are those of Itoh *et al.*,[19] on a Tl 2201 sample which had a $T_c=23$ K. For overdoped systems, the various parameters (α, $\omega_{\rm sf}$, ξ) which determine the spin-fluctuation spectrum do not vary appreciately with the doping level; hence our use of parameters chosen to fit the NMR experiments of Itoh *et al.* should not produce an appreciable error. In choosing band structure parameters for our calculation, we assumed the band structure for the Tl system is close to that found in BSCCO family. Our calculated results, are compared with experiment in Fig. 5. We present our results only for $T>100$ K, since for $T \ll 100$ K the stability of our numerical solution becomes questionable. Clearly the fit is quite good; both theory and experiment show that the system crosses over from the quadratic to linear in frequency behavior at a frequency πT_0, which is of order $\omega_{\rm sf}\xi^2(\Delta k)^2_{\rm max}/2=40$ meV. Note that the crossover behavior changes very little with temperature, as

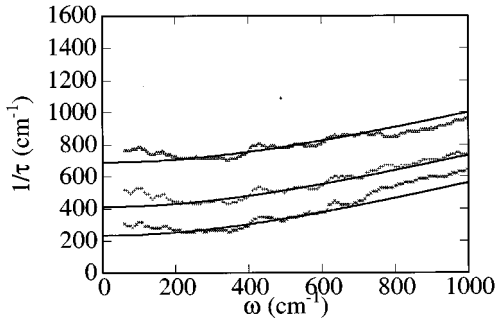

FIG. 5. A comparison of the calculated scattering rate as a function of ω in Tl 2201 with the experimental results of Puchkov *et al.* (Ref. 1). The curves correspond (from bottom to top) to $T=120$ K, 200, and 300 K, respectively. The theoretical curves were obtained using spin-fluctuation parameters appropriate for this material, $\omega_{\rm sf}=[12+0.003\,T\ ({\rm K})]$ meV and $\omega_{\rm sf}\xi^2=50$ meV. The FS size was estimated from the ARPES results on the closely related BSCCO compounds, for which $\Delta k_{\rm max}\approx 1.4$. The coupling constant g^2 was adjusted to yield the correct spread of the curves at $\omega=0$ and a constant term was added, to take into account the likely presence of imperfections in the samples.

predicted by Eq. (23) for the case of the $z=2$ scaling present in all (sufficiently) overdoped materials. We further note that only two fitting parameters appear in our calculation: the coupling constant g and the zero-frequency offset [which is very small, $1/\tau(\omega=0)\sim 30\ {\rm cm}^{-1}$ and is likely generated by impurities]. If the resistivity were measured for this material, both fitting parameters would be fixed by experiment.

In Fig. 6 we compare our calculated optical conductivity for optimally doped $YBa_2Cu_3O_7$ with the experimental results of Ref. 20. We have assumed, as in previous work, that $\omega_{\rm sf}=[6+0.06\,T\ ({\rm K})]$ meV, $\omega_{\rm sf}\xi^2=60$ meV. Strictly speaking, this scaling law, applicable only for temperatures above $T_{\rm cr}\sim 140$ K, is only approximately correct at lower temperatures. At high temperature our calculated results agree quite

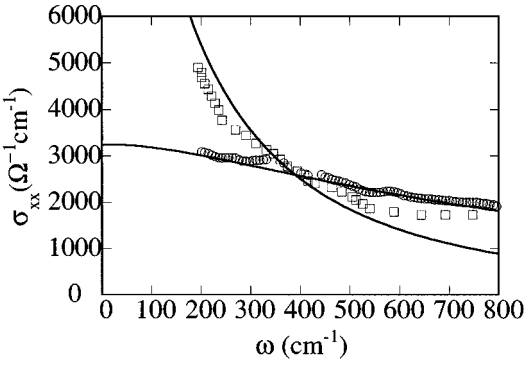

FIG. 6. A comparison of the calculated optical conductivity of $YBa_2Cu_3O_7$ with the experimental results of Tanner *et al.* (Ref. 20). The top curve and the circles correspond to $T=100$ K and the bottom curve and the squares correspond to $T=300$ K. The parameters are those used earlier (Ref. 9), $\omega_{\rm sf}\xi^2=60$ meV, $\omega_{\rm sf}=[6+0.06\,T\ ({\rm K})]$ meV, with $t=250$ meV and $t'=-0.4t$. Just as was the case for the resistivity, agreement with experiment is much better at higher temperatures. The value of the coupling constant g used here, $g=0.6$ eV, is somewhat larger than $g=0.53$ eV used in Ref. 9 to fit the resistivity, ρ_{xx}.

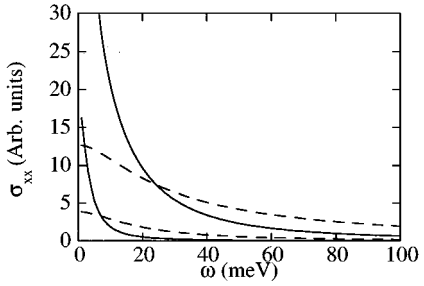

FIG. 7. Schematic behavior of a system with strong a-b plane anisotropy, such as $YBa_2Cu_4O_8$ material. The lower (upper) curve corresponds to σ_{aa} (σ_{bb}), with the solid (dashed) line referring to $T=100$ K ($T=300$ K). The input parameters ($\omega_{sf}=[2+0.02\,T\ (\mathrm{K})]$ meV, $\omega_{sf}\xi^2=60$ meV, $t_a=0.55t_b$) are the same as in Fig. 22 of Ref. 9. Clearly, both the magnitudes and the qualitative behavior of the two conductivities are different: σ_{bb} is far more FL-like than is σ_{aa}.

well with the experiment, both qualitatively and quantitatively. At low T qualitative agreement is found; the calculated $\sigma_{xx}(\omega)$ at $T=100$ K crosses the calculated $\sigma_{xx}(\omega)$ at $T=300$ K at roughly the same frequency as that seen experimentally, although at high ω the calculated values of σ_{xx} are considerably lower than those seen experimentally. We attribute this discrepancy, in part, to the possible presence of disorder in the experimental samples: For example, we found it necessary to use a higher value of the coupling constant g ($g\approx 0.6$ eV) than that used in Ref. 9 ($g\approx 0.5$ eV) to fit the resistivity. A small amount of, e.g., impurity scattering can bring about significant changes in transport and optical behavior at relatively low temperatures, while producing a negligible effect at higher T.

An interesting feature of the $YBa_2C_xO_y$ family is the a-b plane anisotropy, which is seen in untwinned single crystals near optimal doping. (We have earlier provided a qualitative explanation for the anisotropy in the resistivity of these materials[9] and it is instructive to consider its optical counterpart.) In Fig. 7 we show the optical conductivity for a model system which displays strong a-b planar anisotropy, comparable to that observed in $YBa_2Cu_4O_8$. We follow Ref. 9 and assume that the main influence of the CuO chains is to modify the electronic properties of the a-b plane and so model the observed anisotropy by introducing anisotropic hopping matrix elements along the two different crystallographic directions, with $t_a=0.55t_b$. This value of t_a is somewhat low, but is not unreasonable for a qualitative analysis for pedagogical purposes. The input parameters ($\omega_{sf}=[2+0.02\,T\ (\mathrm{K})]$ meV and $\omega_{sf}\xi^2=60$ meV) are the same as in our earlier work.[9] As can be seen from the figure, the strong anisotropy we found for the dc resistivity has its analog in the case of $\sigma_{xx}(\omega)$, as might have been expected; the strongly conducting a direction displays a distinctly different ω dependence at higher frequencies. This behavior can be understood by recalling that when the current runs along the a direction, the distribution of hot spots is such as to yield scattering rates which are mostly FL-like, and hence one should expect to see a large conductivity even at large ω. On the other hand, for current running along the b direction the dominant contribution to the conductivity comes from quasiparticles which possess strongly anomalous scattering rates; this leads to a much stronger frequency dependence of $\mathrm{Re}\sigma_{bb}(\omega)$, of the kind observed in many underdoped samples.

We consider next the underdoped materials. Above T_*, we expect the behavior of $1/\tau_{\mathrm{eff}}$ to take the MFL form, Eq. (25). Indeed, Eq. (25), obtained for a moderately large FS, does not depend on the spin-fluctuation parameters ω_{sf} and ξ and hence independent of the scaling law relating ω_{sf} and ξ; $1/\tau_{\mathrm{eff}}$ is linear in both T and ω both above and below T_{cr}, as long as $T>T_*$. On the other hand, it is now widely believed that in heavily underdoped materials, below T_*, the hot quasiparticles, which are close to the magnetic BZ boundary become effectively gapped (the pseudogap), with much of the quasiparticle weight transferred from low to high frequencies; the quasiparticle band dispersion thus acquires a form similar to that encountered with a preformed spin-density-wave (SDW) state.[8] Hence, at low frequencies, hot quasiparticles barely contribute to transport, a conclusion which is consistent with the superfluid density measurements at low temperatures, which suggest that only a fraction of the doped holes become part of the superconducting condensate.[14,21] Although quasiparticles are not well defined in the hot region of the BZ, since their quasiparticle residua are rather small, they still contribute to transport up to frequencies of order T_*. Above this scale their scattering is so strong that $\mathrm{Im}\Sigma$ is essentially temperature and frequency independent (see the result for $\Delta k=0$ in Fig. 2). On the other hand, the cold quasiparticles are still well defined, albeit in a somewhat narrower region, centered around $\mathbf{k}=(\pi/2,\pi/2)$, and symmetry-related points in the Brillouin zone. However, since so much of the FS is gapped, the phase space available for the scattering of cold quasiparticles is considerably reduced. Thus, for small frequency $\omega<T_*$, one expects $1/\tau_{\mathrm{eff}}\propto\omega^2$, just as one finds $1/\tau\sim T^2$ at zero frequency and temperatures well below T_* in underdoped materials. In other words, there is a significant temperature variation of $1/\tau_{\mathrm{eff}}$ up to this frequency. As the hot quasiparticles cease to contribute to transport above this energy scale, which is valid as long as the correlation length is large (that is, for $\xi\geqslant 2$ and $T<T_{cr}$), the slope of $1/\tau_{\mathrm{eff}}$ is reduced and it acquires its usual linear in ω dependence. In terms of the NAFL model, a close study shows that the effective rate $1/\tau_{\mathrm{eff}}(\omega)$ increases up to frequencies of order $T_*\sim\omega_{sf}\xi^2(\Delta k)^2_{\mathrm{max}}/2$, where Δk_{max} is much smaller (~ 0.1–0.5) than is found in optimally doped materials. This phenomenon is the optical analog of the resistivity which is a considerably stronger function of temperature below T_* than above it. It is noteworthy that at sufficiently high temperature, above T_{cr}, much of the quasiparticle weight is again transferred to the low frequencies and the hot quasiparticle again start to contribute to transport, but the slope of $1/\tau_{\mathrm{eff}}$ does not change, since it does not depend on the scaling law between the spin fluctuation parameters.

We note that the fact that the contribution of the hot regions is strongly reflected in experiment in the underdoped materials suggests that large parts of the FS are in fact hot. Moreover, at higher frequency and low temperatures the slope of $1/\tau_{\mathrm{eff}}$ is the same as that found at high T in systems where there is no pseudogap present. If large parts of the FS exhibit highly anomalous behavior, then one should expect that at relatively low frequencies $1/\tau_{\mathrm{eff}}$ would begin to satu-

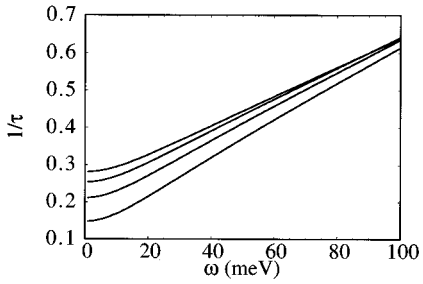

FIG. 8. $1/\tau_{\rm eff}$, obtained for a small FS, $\Delta k_{\rm max}=0.4$, by numerically solving Eqs. (17) and (26), for the same input parameters as in Fig. 4, but adding a FL scattering contribution, $V_{\rm FL}=\chi_0/(1-\imath\pi\omega/\Gamma)$, with $\Gamma=400$ meV, to the magnetic interaction, Eq. (4). The curves correspond (bottom to top) to $T=100$, 150, 200, 250 K. At high frequency the averaged quasiparticle lifetime is nearly T and ω independent, in accordance with experiment on the underdoped materials. The stronger temperature dependence at low frequency stems from the strongly temperature-dependent spin-fluctuation spectrum found in all underdoped materials.

rate. Indeed, we have found that the MFL form of $1/\tau_{\rm eff}$, Eq. (25), is obtained only for a large FS, while for a smaller FS one would expect $1/\tau_{\rm eff}$ to display sublinear behavior as a function of frequency. This suggests that the linear-in-ω behavior of $1/\tau_{\rm eff}$ above T_* reflects scattering processes involving momentum transfers far from **Q**, which supplement the magnetic scattering we have considered. If one is to maintain the linear behavior of $1/\tau_{\rm eff}$ for πT and ω larger than $\omega_{\rm sf}\xi^2$, the dominant scattering mechanism must crossover from processes involving small to those involving larger characteristic frequencies. For example, in Ref. 9 we introduced FL scattering in order to avoid resistivity saturation at higher temperatures in 214 systems and obtained thereby quite reasonable agreement with experiment near optimal doping level. In this respect, optimally doped materials are merely those which have the smoothest transition from low-energy to high-energy scales, in excellent agreement with the experimental findings of Takagi *et al.*[22]

The additional scattering processes introduced to maintain linear in frequency $1/\tau_{\rm eff}$ above the pseudogap scale do not qualitatively change the behavior of the effective relaxation rate at low frequencies which is still governed by the strong magnetic scattering. We present in Fig. 8 the result of a numerical calculation of $1/\tau_{\rm eff}$, where we have used $\Delta k_{\rm max}=0.4$, taken $\omega_{\rm sf}$ and ξ to be the same as in Fig. 4(a), and have incorporated in our numerical work, based on Eqs. (26) and (27), a FL-like scattering potential $V_{\rm FL}=\chi_0/(1-i\pi\omega/\Gamma)$, where $\Gamma=400$ meV. Notice that $1/\tau_{\rm eff}$ loses its temperature dependence at high frequency; i.e., all curves shown in the figure converge at a frequency $\sim\omega_{\rm sf}\xi^2(\Delta k_{max})^2/2$. Below this frequency $1/\tau_{\rm eff}$ displays considerable temperature dependence, even though we have not included the increase of $\omega_{\rm sf}$ at low temperatures and a possible temperature variation in the effective size of the FS. Within the magnetic scenario, these scattering processes are closely related to the experimentally measured energy scales for $\mathbf{q}\approx\mathbf{Q}$. Moreover, since the scale of $\omega_{\rm sf}\xi^2$ is weakly doping dependent and always of the order of $1/\pi$ times the Fermi energy the crossover energy should be almost material independent, in agreement with NMR experiments which show that for most materials $\xi(T_{\rm cr})\approx 2$.

VI. CONCLUSION

In summary, we have applied both analytical and numerical techniques to the study of the transport properties of HTS's at optical frequencies within the NAFL model. We find that the peaking of the effective magnetic interaction leads to strong anisotropy of the quasiparticle properties in different regions of the BZ, and brings about a complex morphology for the optical conductivity and the effective scattering rate $1/\tau_{\rm eff}(\omega)$, which can be extracted from it. We found that for a wide region of temperature and frequencies the NAFL model leads directly to the MFL form for $1/\tau_{\rm eff}$, Eq. (25), a scattering rate which agrees with experimental results found in nearly all optical measurements to date. Overall, in the appropriate limits, our results agree qualitatively and many cases quantitatively, with the experimental findings.

In this paper we have focused on the optimally doped and overdoped materials. In the underdoped case, to obtain results of comparable quality, one must parametrize in some detail changes in the quasiparticle behavior brought about by the quasiparticle pseudogap, which we have not yet done. However, to the extent that the FS undergoes a substantial transition as one varies doping from optimal to underdoped we have shown that the magnetic scenario provides results in qualitative agreement with experiment, even within this simple theory.

Our use of the Born approximation, would seem to work somewhat better than one would expect it to in a system with strong correlations. Ideally, one should obtain $\Sigma(k,\omega)$ self-consistently, before substituting it into Eq. (27). However, it may prove easier to calculate the current-current correlation function directly.[23] The results of calculations which include both the pseudogap and strong coupling effects will be presented in forthcoming publications.[24,25]

ACKNOWLEDGMENTS

We are indebted to G. Blumberg, G. Boebinger, A. Chubukov, D. Ginsberg, P. Monthoux, T. M. Rice, J. Schmalian, Q. Si, C. Slichter, R. Stern, and T. Timusk for stimulating conversations on these and related topics. We should like to thank Tom Timusk for his helpful remarks following a critical reading of an earlier version of this manuscript. We thank the National Center for Supercomputing Applications for a grant of computer time. This research has been supported in part by NSF through Grant No. NSF-DMR 89-20538 (MRL at UIUC) and NSF-DMR 91-20000 (STCS).

*Present address: Center for Nonlinear Studies, Los Alamos National Lab., Los Alamos, NM 87545.

†Permanent address: Department of Physics and Materials Research Laboratory, 1110 West Green Street, University of Illinois, Urbana, IL 61801.

[1] A. V. Puchkov, D. N. Basov, and T. Timusk, J. Phys.: Condens.

Matter **8**, 10 049 (1996), and references therein.
[2] P. W. Anderson, *The Theory of High Temperature Superconductivity in the High-T_c Cuprate Superconductors* (Princeton University Press, Princeton, 1997).
[3] C. M. Varma, P. B. Littlewood, S. Schmitt-Rink, E. Abrahams, and A. E. Ruckenstein, Phys. Rev. Lett. **63**, 1996 (1989).
[4] G. Kotliar *et al.*, Europhys. Lett. **15**, 655 (1991).
[5] A. G. Loeser *et al.*, Science **273**, 325 (1996).
[6] Recent reviews of the NAFL approach may be found in D. Pines, Physica C **235-240**, 113 (1994); in *High-Temperature Superconductivity and the C^{60} Family*, edited by H. C. Ren (Gordon and Breach, New York, 1995), pp. 1–32.
[7] R. Hlubina and T. M. Rice, Phys. Rev. B **51**, 9253 (1995); *ibid.* **52**, 13 043 (1995).
[8] A. V. Chubukov and D. Morr, Phys. Rep. (to be published) and references therein.
[9] B. P. Stojković and D. Pines, Phys. Rev. B **55**, 8576 (1997).
[10] A. J. Millis, H. Monien, and D. Pines, Phys. Rev. B **42**, 167 (1990).
[11] A. V. Chubukov, D. Pines, and B. P. Stojković, J. Phys.: Condens. Matter **8**, 10 017 (1996).
[12] V. Barzykin and D. Pines, Phys. Rev. B **52**, 13 585 (1995); Y. Zha, V. Barzykin, and D. Pines, **54**, 7561 (1996).
[13] J. Schmalian (private communication).
[14] P. Monthoux and D. Pines, Phys. Rev. B **50**, 16 015 (1994); D. Pines, in Proceedings of Evora Conference on Unconventional Fermi Liquids [Z. Phys. B **103**, 129 (1997)].
[15] B. P. Stojković, Philos. Mag. B **74**, 529 (1996).
[16] See, e.g., C, P. Slichter, in *Strongly Correlated Electronic Materials*, edited by K. S. Bedell *et al.*, (Addison-Wesley, Reading, MA, 1994); N. Curro *et al.*, Phys. Rev. B **56**, 877 (1997).
[17] G. Rickayzen, *Green's Functions and Condensed Matter Physics* (Academic Press, London, 1980).
[18] S. V. Shulga, O. V. Dolgov, and E. G. Maksimov, Physica C **178**, 266 (1991).
[19] Y. Itoh *et al.*, J. Phys. Soc. Jpn. **63**, 22 (1994).
[20] D. Tanner *et al.*, J. Supercond. **8**, 563 (1995).
[21] F. Gao *et al.*, Phys. Rev. B **54**, 700 (1996).
[22] H. Takagi *et al.*, Phys. Rev. Lett. **69**, 2975 (1992).
[23] P. Monthoux and D. Pines, Phys. Rev. B **47**, 6069 (1993); **49**, 4261 (1994), and references therein.
[24] J. Schmalian *et al.* (unpublished).
[25] V. Roubtsov *et al.* (unpublished).